BILINGUAL PUBLISHING CO.
Pioneer of Global Academics Since 1984

Journal of Geological Research
https://ojs.bilpublishing.com/index.php/jgr-a

ARTICLE

AIRRLS: An Augmented Iteratively Re-weighted and Refined Least Squares Algorithm for Inverse Modeling of Magnetometry Data

Maysam Abedi*

Geo-Exploration Targeting Lab (GET-Lab), School of Mining Engineering, College of Engineering, University of Tehran, Tehran, Iran

ARTICLE INFO

Article history
Received: 18 October 2019
Accepted: 21 November 2019
Published Online: 31 December 2019

Keywords:
l_p norm problem
AIRRLS algorithm
3D inversion
Magnetic anomaly
Porphyry mineralization

ABSTRACT

This work aims to examine the functionality of a new Augmented Iteratively Re-weighted and Refined Least Squares algorithm (AIRRLS) to generate a 3D model of magnetic susceptibility property from a potential field magnetometry survey. Whereby this algorithm ameliorates an lp norm Tikhonov regularization cost function through replacing a set of weighted linear system of equations. It leads to constructing a magnetic susceptibility model that iteratively converges to an optimum solution, meanwhile the regularization parameter performs as a stopping criterion to finalize the iterations. To tackle and suppress the intrinsic tendency of a sought target responsible for generating a magnetic anomaly and to not be imaged at shallow depth in inverse modeling, a prior depth weighting function is imposed in the principle system of equations. The significance of this research lies in improvement of the performance of the inversion, where the running time of an lp norm problem after incorporating a pre-conditioner conjugate gradient solver (PCCG) in cases of large scale geophysical dataset. Forasmuch as this study attempts to image a geological target with low magnetic susceptibility property, it is assumed that there is no remanent magnetization. The applicability of the algorithm is tested for a synthetic multi-source data to demonstrate its performance in 3D modeling . Subsequently, a real case study in Semnan province of Iran, is investigated to image an embedded porphyry copper layer in a sequence of sediments. The sought target consists of a concealed arc-shaped porphyry andesite unit that may have potential of Cu occurrences. Results prove that it extends down at depth, so exploratory drilling is highly recommended to get insights about its potential for Cu-bearing mineralization.

1. Introduction

One of the notable problems in the varied fields of applied geophysics is the inverse modeling of the ill-posed system of equations as a forever field of active research. Inverse modeling of geophysics data is usually ill-posed/conditioned which means that the solution models not only depend on the observations, but also require supplementary prior pieces of information (e.g., geological characteristics) to be imposed in the cost

**Corresponding Author:*
Maysam Abedi,
Geo-Exploration Targeting Lab (GET-Lab), School of Mining Engineering, College of Engineering, University of Tehran, Tehran, Iran;
Email: MaysamAbedi@ut.ac.ir

DOI: https://doi.org/10.30564/jgr.v1i3.1316

function to generate unique and stable outputs. From a geophysical standpoint, this issue is more sensible when modeling physical properties of the magnetic susceptibility or density contrast from potential field geophysical data [20,46]. Several studies have been dedicated to acquire a reasonable solution in the geophysical inverse modeling, in all of which the following conditions are inevitable. Non-uniqueness of the generated models which means that the geophysical problem has infinitely many solutions because of the under determined system of equations. Instability of the models which means that the inverse modling leads to unstable solutions for the sake of low values of the eigenvalues in the forward kernel or sensitivity operator. Care must be taken that a noisy observation is also another permanent source of model instability [4,19].

Potential field magnetometry data has investigated by many geoscientists to model the magnetic property and geometry of causative sources. The inversion procedure of such a dataset is generally divided into two categories that are (1) parametric inversion, and (2) physical property inversion as a tremendously important part of inverse modeling. The parametric methods are usually suitable for pre-assumed cases that are easily simulated by a simple-shaped causative source. Here, an appropriate geological model is assumed to fit the potential field observations by attempting a human-computer interaction (e.g. [1-3,10,15-17]). The later methods with higher favorability and flexibility are full automatic and iterative, where the generated models have a physical contrast with the background geological setting of the prospect zone [46]. Physical-based inversion methodologies are designed on the basis of an appropriate model cost function, and it is actually rather difficult to implement rather than the parametric one.

Extensive efforts have been dedicated to deal with full automatic inversion of potential field geophysical data. Among various researchers designed, Last and Kubik [23] proposed a compact inversion scheme to correctly construct sharp borders of the sought sources. As the first spark for defining a new approach in inverse modeling of potential field data, Li and Oldenburg [28] discussed a novel technique for 3D recovering of physical properties by minimizing a global Tikhonov cost function with constituent norms of a model stabilizer and a data misfit simultaneously. It's worth pointing out that a depth weighting function was also proposed to avoid the intrinsic decay of the potential field geophysical data at depth, where they have assigned higher weights to the deeper cells of discretized model domain. Following the same line of thought as Li and Oldenburg [28], depth weighting has been imposed in the proposed methodologies for correct recovering of geophysical models of the magnetic susceptibility and the density contrast (e.g., [4,6,8,11,12,14,26,27,30,31,33,34,35,36,38]).

An iteratively re-weighted least squares algorithm (IRLS) is a possible scenario to strive for high speed inversion of geophysical data and other fields of mathematical computation for solving the discrete ill-posed equations. Incorporating an iterative refinement strategy which is known as an iteratively re-weighted and refined least squares (IRRLS), has tackled significantly the high computational burden of the conventional IRLS [18]. The efficiency of this algorithm has been successfully examined for synthetic seismic data (i.e., a vertical seismic profiling, a sparse spike deconvolution and a cross-well seismic tomography) for solving linearized inverse problems [18]. Herein, this algorithm is augmented by incorporating a depth weighting function and a pre-conditioner conjugate gradient tool (PCCG) to solve an l_p norm problem by a set of weighted linearized equations in order to iteratively retrieve magnetic susceptibility property from the magnetic field anomalies. A synthetic multi-source magnetic data along with a real airborne magnetic data are used in later sections to investigate its performance in inverse modeling of the magnetometry data.

Airborne geophysical survey is a fruitful tool in exploration of various porphyry-type ore mineralization such as Cu and Mo deposits, being used worldwide in the reconnaissance phases of exploration programs. Partitioning of iron between oxides and silicates in generic model of porphyry-type systems often impacts on magnetic characteristics of intrusive magmatic units and host rocks [13]. Note that hydrothermal alterations in association with such reservoirs can fluctuate the magnetic signatures of sought targets due to their sulfide contents [21]. Since alteration zones are localized on the center of causative source, they are usually distinguished through reflecting a desired geophysical response of magnetic anomaly. Regional magnetic field intensity amplifies over the potassic alteration, but it reduces over the sericitic zone. This magnetic signature partially intensifies over the propylitic zone which usually surrounds the sought target [43]. Such a geophysical footprint can facilitate the prospecting of porphyry-type resources in airborne magnetometry survey.

This work aims to investigate the mining potential of a geological unit that may be a host of porphyry Cu mineralization. Thus, the airborne magnetometry data surveyed at the Kalat-e-Reshm area in Semnan province of Iran, are taken as a real case study into account to image the magnetic susceptibility property of the desired sought target. It's worth pointing out that the analyzed helicopter borne electromagnetic data over this area have proved the

 DOI: https://doi.org/10.30564/jgr.v1i3.1316

occurrence of an arc-shaped porphyry andesite rock with higher electrical resistivity encircled by a thick sedimentary setting. The occurrence of this unit has been confirmed by ground and airborne surveys of direct current electrical resistivity and airborne magnetometry data as well [39-42]. Forasmuch as the sought target has a sharp magnetic signature, its magnetic susceptibility model can provide insightful information about the intensity of hydrothermal alterations, intrusive magmatic and porphyry unit (e.g. [32]). Therefore, the aeromagnetic data of this area were revisited to apply and appraise the functionality of the proposed AIRRLS algorithm in 3D inverse modeling of magnetic susceptibility property.

The remainder of this work has been prepared as follows. In the second section, the forward and inverse modeling of the magnetic field data are mentioned and the system of equations for solving an ill-posed problem through the proposed AIRRLS algorithm is discussed in details. The performance of the algorithm is examined for a synthetic data in the section three. In fourth section, the geological setting of the sought target is concisely explained. Airborne magnetometry data are inverted in the section fifth to construct the geometry of the andesite unit in the Kalat-e-Reshm prospect zone. Finally, the main achievements are summarized in the conclusion.

2. Methodology

To invert the potential field magnetic data, the desired model domain can be discretized into a structural regular mesh through defining a set of rectangular prisms to cover a complicated geometry. In case of considering a small mesh size, each cell is usually assumed with a constant magnetic susceptibility value. Note that a linear system of equation can project the magnetic susceptibility property into a magnetic anomaly data domain when low magnetic susceptibility amounts exist for the causative magnetic source. It offen happens for most porphyry-type sources. Thus, it leads to a simplified linear system of equation in inverse modeling [31]. In addition to this simplification, the assumption of no remanent magnetization of the causative sources in the porphyry type deposits works well. A comprehensive and precise ideas to cope with this issue can be found in the works by Lelièvre and Oldenburg [24], and Li et al. [25].

For ease of notation in this work, the small letters with bold font are used to introduce a vector and its components x_i, i.e., $x=(x_1,x_2,...x_m) \in R^m$. Likewise, the bold and capital letter as G defines a matrix. The value of a variable at the lth iteration as $(.)^l$, e.g., x^l, shows the model solution at this iteration. Finally, x^* is the converged and optimum model solution.

2.1 Forward Modeling

The forward equations of the potential field magnetic data after introducing by Bhattacharyya [9], were casted in a more facile form to raise its utilizability in in computer coding [37]. Magnetic anomaly arising from an m cells is calculated at a coordinate (x, y, z) through the following equation,

$$\Delta t\left(x,y,z\right)=\sum_{j=1}^{m}\Delta t_j\left(x,yxz\right)+c, \tag{1}$$

where Δt is the total magnetic data overlaid by c as a regional magnetic trend [37]. Assuming that there are n observations from m cells, Eq. (1) is simplified by the matrix notation as the following linearized form,

$$t=Gx, G\in R^{n\times m}, x\in R^m, t\in R^n \tag{2}$$

where t is the magnetic observation vector after detrending a regional c constant, G is the forward sensitivity kernel which projects from the physical model space to the magnetic observation space. Here, x is a vector of the sought magnetic susceptibilities.

2.2 Inverse Modeling

For the sake of the intrinsic instability arising from a linear operator G, a regularized solution must be searched in the magnetometry studies [14]. Various inversion methodologies have been developed to regularize and stabilize the inverse problems in all fields of mathematically computations, where among them geophysical communities have had significant impact on this topic [44,45].

In potential field geophysical context, a Gaussian noise distribution with zero mean and finite variance of σ^2 is assumed for noise-corrupted magnetic observations. To extract a suitable model of the magnetic susceptibility distribution x in Eq. (2), the system of equation can be replaced by a well-posed l_p norm cost function as,

$$l_p\left(x,\delta\right)=\min_{x\in R^m}\frac{\lambda}{2}\left\|t-Gx\right\|_2^2+\sum_{i=1}^{m}\left(\left(Lx\right)_i^2+\delta\right)^{p/2} \tag{3}$$

where δ is a small value and λ works as a regularization tool [29]. Since λ is unknown, it is essential to search its optimum value through a posterior rule. It leads to multiple running of the algorithm for a range of λ's regularization values to pick up an optimum constant in association with the best constructed model. This kind of processing is time consuming and somewhat arbitrary, so the regularization and minimization of the above mentioned cost function become a tough task in inverse modeling of potential field geophysical data. The later section discusses in details how it is searched

DOI: https://doi.org/10.30564/jgr.v1i3.1316

in the proposed AIRRLS algorithm [18]. The operator L presents the n*th*-order derivatives in x, y, and z directions to adjust the smoothness and roughness of the sough model.

An iteratively re-weighted least squares method (IRLS) was employed by Lai and Wang [22] to solve Eq. (3) as follows,

$$\left(\lambda G^T G + L^T S^l{}_x L\right) x^{l+1} = G^T t \tag{4}$$

and with imposing the iteratively updated weights as

$$S_x^l = diag\left(\frac{p}{\left(\delta + \left(x_i^l\right)^2\right)^{1-\left(\frac{p}{2}\right)}}\right) \tag{5}$$

The original formulation of the IRLS algorithm needs solution of a re-weighted system of linear equations several times to reach an optimum solution x^* . The iteration number is equivalent to the multiplied numbers of three terms that are the number of λ'*s* (for updating weights), the number of iterations for searching , and the CG iterations. In the following section, the AIRRLS method proposed by Gholami and Mohammadi Gheymasi [18] is adopted to an l_p norm problem in the magnetometry study on the basis of a refinement strategy by which the iteration number decreases to λ'*s*×*CG* iterations.

2.3 The AIRRLS Method

Following the same line of thought as Gholami and Mohammadi Gheymasi [18], the AIRRLS is utilized here to solve the defined Tikhonov cost function (Eq. 3) with two terms-that are a regularized model norm and a misfit norm. A nonstationarity weighting matrix, Q, was defined by being iteratively refined to solve the equation via the following formulations,

$$x^{l+1} = ax^l + Q_{x^l}\left(t - \alpha G x^l\right) \tag{6}$$

$$Q_{x^l} = \lambda^l \left(\lambda^l G^T G + L^T S_x^l L\right)^{-1} G^T \tag{7}$$

where 0≤α≤1. Smaller α values correspond to lower impact of refinement. The main advantage of the nonstationary method is originated from updating the Tikhonov regularization parameter λ successively and iteratively as λ^l. A possible scenario to investigate a predefined range of regularization parameters is searching for the following increments of $\lambda^l[\lambda_{min}, \lambda_{max}]$,

$$\lambda^l = \lambda_{\min}\left(\lambda_{\max} / \lambda_{\min}\right)^{l/N} \tag{8}$$

where N is the iteration number of the AIRRLS algorithm.

Efficiently running the AIRRLS algorithm for cases of large scale magnetic observations requires consideration of a fast solver for the central system of Eq. (7). It is a tough task to solve it explicitly through direct solvers, so iterative methods such as a CG algorithm can be a panacea with high convergence rate when incorporating a pre-conditioner. A diagonal pre-conditioner is substituted in the center of the AIRRLS algorithm to augment the solver by imposing,

$$M = diag\left(\lambda^l G^T G + L^T S_x^l L\right) \tag{9}$$

To compensate the lack of sensitivity of the deeper cells in the discretized model domain when inverting magnetic data, a depth weighting function introduced by Li and Oldenburg [28] is inserted in the inversion equation. It has a form of $(z)=(z+\varepsilon)^{-\beta/2}$, where β is the structural index of a magnetic source, and ε constant depends on the altitude of observations to prevent singularity for cases with zero values of z [12]. This function is casted in the form of a matrix $Z=diag(W(z))$ for the original system of Eq. (3) by setting $G_Z=GZ^{-1}$ and $k=Z_x$. After solving the problem for k, the final magnetic susceptibility model is obtained from $x=Z^{-1}k$. A pseudo code for running the AIRRLS algorithm has been summarized in Table 1.

Table 1. The summary of the AIRRLS algorithm for inverse modeling of the magnetic field data

Initialize;
Input: λ_{min}, λ_{max}, α, δ, p, ε, β, CG iteration, and number of algorithm iterations N
Set: $\lambda^l=\lambda^{min}$,$x^l=0$,$S_x^l=I$, $L=I$
Incorporate: $Z=diag(W(z))$
for $l=1:N$
Compute the residual $r^l=t-\alpha G_z k^l$
Solve reweighted system $(\lambda^l G_Z{}^T G_Z + L^T S_x{}^l L)\Delta k^{l+1}=\lambda^l G_Z{}^T r^l$ by iterations of CG method
Consider a pre-conditioner as $M=diag(\lambda^l G_z{}^T G_z + L^T S_\chi{}^l L)$
Refine the solution $k^{l+1}=\Delta k^{l+1}+\alpha k^l$
Compute $S_k^l = diag\left(\frac{p}{\left(\delta + \left(k_i^l\right)^2\right)^{1-\left(\frac{p}{2}\right)}}\right)$
Update $\lambda^l=\lambda_{min}(\lambda_{max}/\lambda_{min})^{l/N}$
end
Find the optimal solution x^* from $x^*=Z^l k^*$
Finish

3. Synthetic Data Modeling

The AIRRLS algorithm is examined here for a synthetic

 DOI: https://doi.org/10.30564/jgr.v1i3.1316

magnetic anomalies from a model domain simulated by four rectangular bodies embedded in a non-susceptible environment. Table 2 has tabulated the assumed properties of each model. A horizontal slice at the center of the models is shown in Figure 1a. The 3D domain is discretized into 40×40×20=32,000 rectangular cells with a uniform dimension of 2.5×2.5×2.5 m in x, y and z directions, respectively. The inclination and declination angles of the earth's magnetic field are fixed to I=50°, D=2°, respectively, assuming a strength of 47,500 nT. Random Gaussian noise with a standard deviation equal to 3% of the data amplitude is superimposed on the 1600 observations. A regular grid of survey is decorated over a 100m×100m region with a sampling space of 2.5 m in both directions. Noise-corrupted residual magnetic field data have been plotted in Figure 1b.

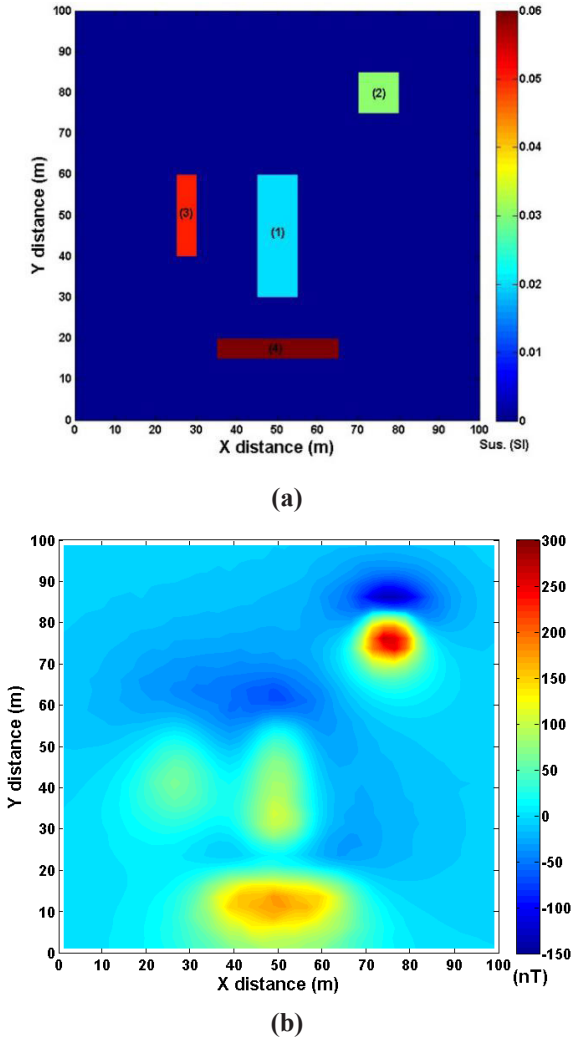

Figure 1. Synthetic magnetic data simulation

Note: (a) a horizontal slice at the center of the multi-source magnetic bodies, on which the numbers correspond to the assumed parameters in Table 1, and (b) the residual total field magnetic data.

Table 2. Characteristics of the simulated magnetic data (similar to the models presented by Abedi et al.[4])

Model Number	x×y×z dimensions (m)	Depth (m)	x (SI)
1	10×30×20	5	0.02
2	10×10×15	2.5	0.03
3	5×20×30	10	0.05
4	30×5×20	7.5	0.06

To run the AIRRLS algorithm for the synthetic data, the value of the refinement coefficient α in Eq. (6) was chosen equal to 1. The structural index β=3 was fixed in the depth weighting function, and as well δ=0.01, ε=0.0001, a zeroth-order roughening matrix L=I, and the l_1-norm for optimization problem were assumed. The regularization interval [λ_{min}, λ_{max}] was searched at an interval of [10^{-17},10^{-14}] for both the synthetic and real case study. The number of algorithm iteration N=500 was chosen to define a range of regularization parameter λ^l according to Eq. (8) by small increment steps. The misfit curve versus the iteration number for the synthetic magnetic data was depicted in Figure 2, indicating gradually converging to an optimal solution in iteration 484. Since the regularization parameters varies at a large interval (with a difference of three order of magnitude), the optimal iteration number was quite large for such a multi-source model in the magnetic data modeling. Note that the PCCG algorithm with 20 iterations was assumed. The running time of an iteration to generate a model was about 4s, meanwhile the PC specifications have components of 4 GHz processor, 64-bit operation system, and 16 GB RAM.

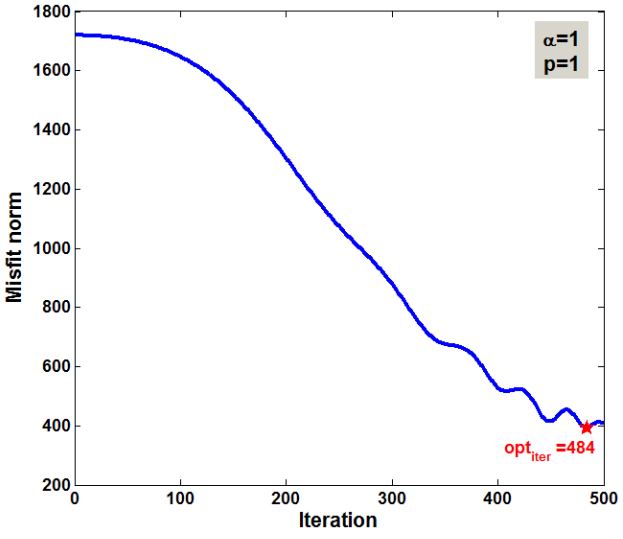

Figure 2. The misfit curve versus the iteration numbers for the synthetic magnetic data. The algorithm converges to an optimum solution at iteration 484

To present the outputs of constructed magnetic suscep-

DOI: https://doi.org/10.30564/jgr.v1i3.1316

tibility model, 3D rendering for various iterations (100, 200, 300, 400, 484, and 500) were respectively depicted in Figure 3, showing gradually convergence to an optimum model at iteration 484. A threshold of 0.005 SI was assumed for the volume rendering of the magnetic susceptibility property in all plots. The relevant predicted magnetic anomalies are also plotted for the aforementioned successive iterations in Figure 4, subsequently by gradually reconstruction of the original magnetic observation shown in Figure 1b.

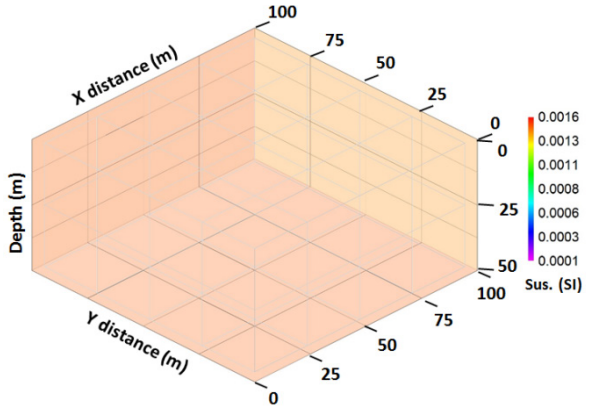

(a)

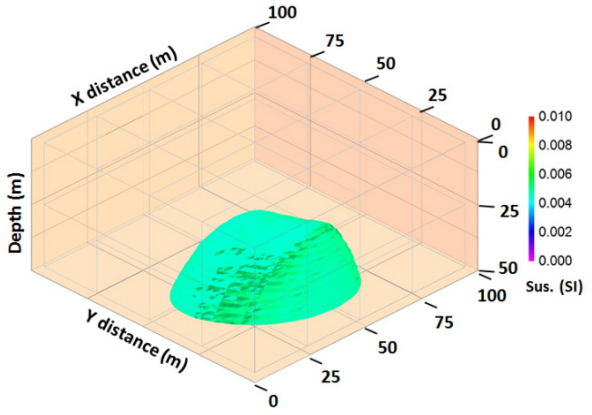

(b)

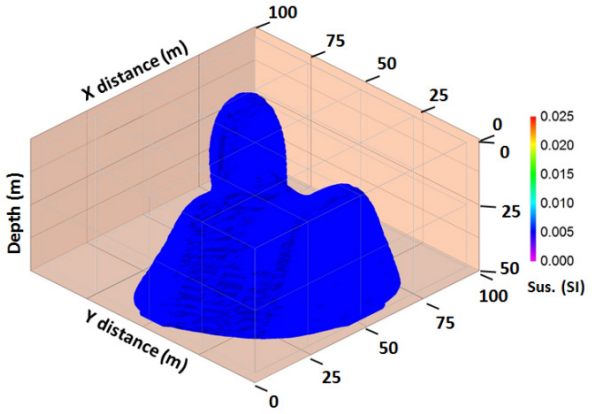

(c)

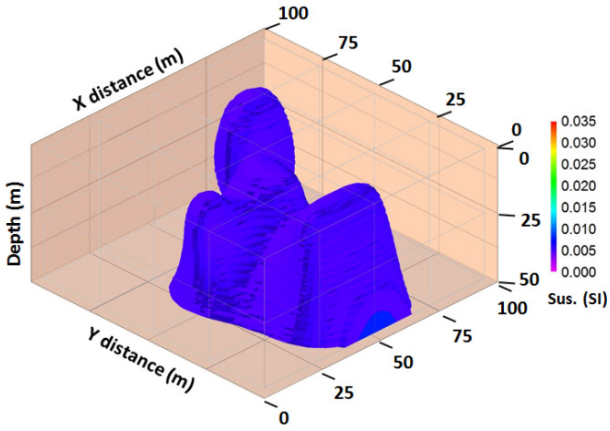

(d)

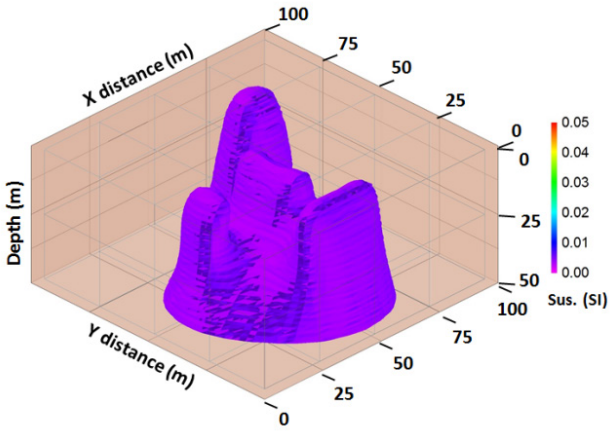

(e)

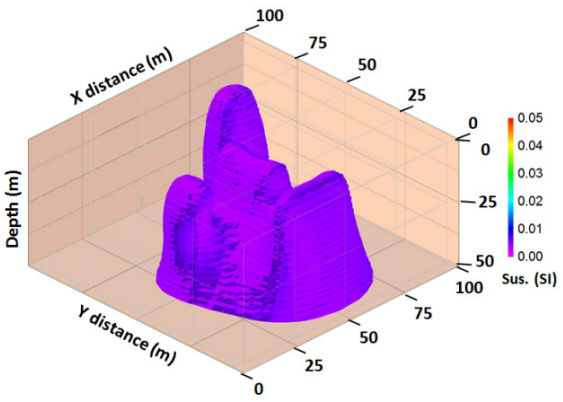

(f)

Figure 3. 3D visualization of the inverted synthetic data for a magnetic susceptibility threshold of 0.005 SI at successive iterations of, (a) 100, (b) 200, (c) 300, (d) 400, (e) 484, and (f) 500

 DOI: https://doi.org/10.30564/jgr.v1i3.1316

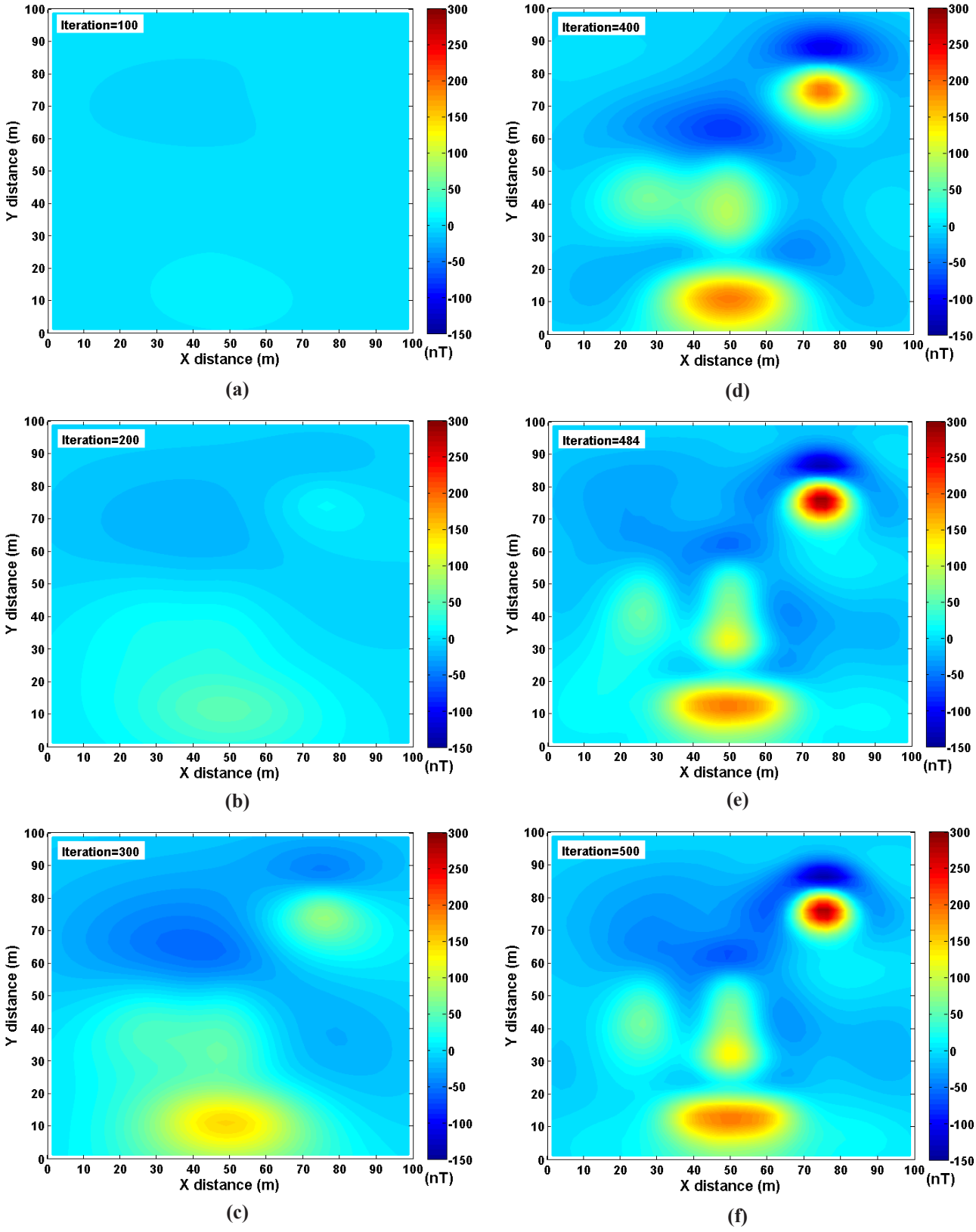

Figure 4. Predicted magnetic data at successive iterations of, (a) 100, (b) 200, (c) 300, (d) 400, (e) 484, and (f) 500

DOI: https://doi.org/10.30564/jgr.v1i3.1316

Four depth slices at different depths of the optimal sought model (Figure 3e) reveal that the simulated multi-source anomalies could be appropriately recovered (Figure 5). The borders of the synthetic sources are superimposed on all indicated maps to better compare the efficiency of the proposed algorithm for magnetic data modeling. A vertically E-W slice along the route with *Y*=50m was plotted in Figure 6. The magnetic susceptibility property across this route is in close consistency with the two synthetic sources. To better visualize the misfit of the predicted magnetic data in optimal iteration number, the scatter plot of the predicted observations versus the synthetic ones is portrayed in Figure 7, where the plotted line is a gauge for determining the overestimated and underestimated data.

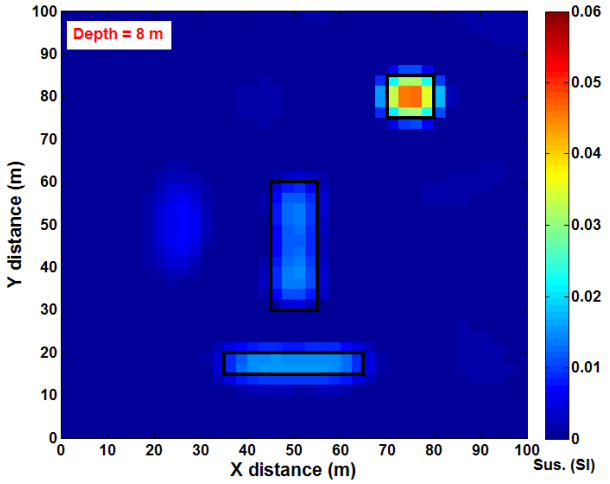

(a)

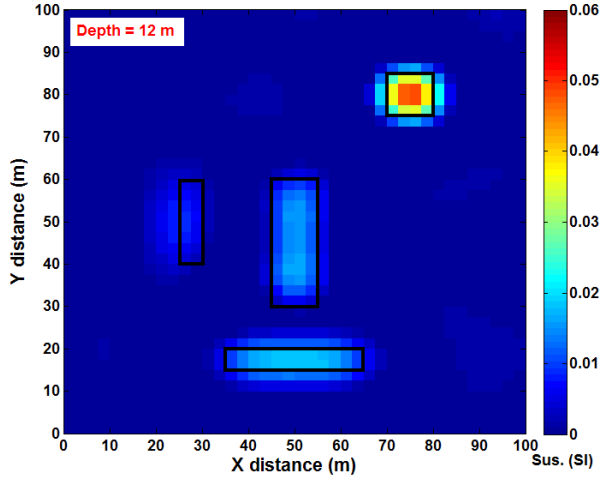

(b)

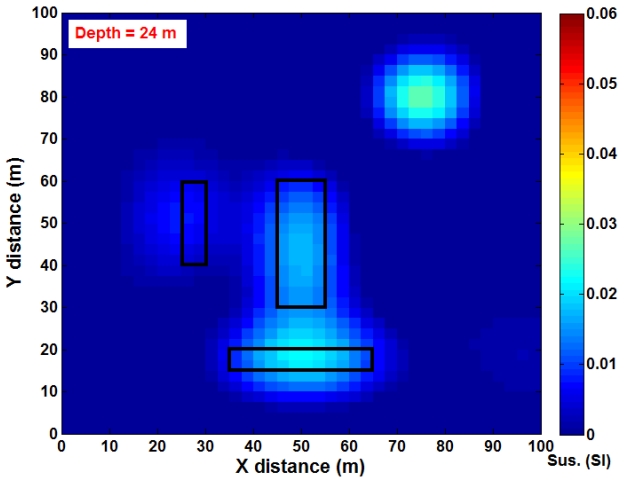

(c)

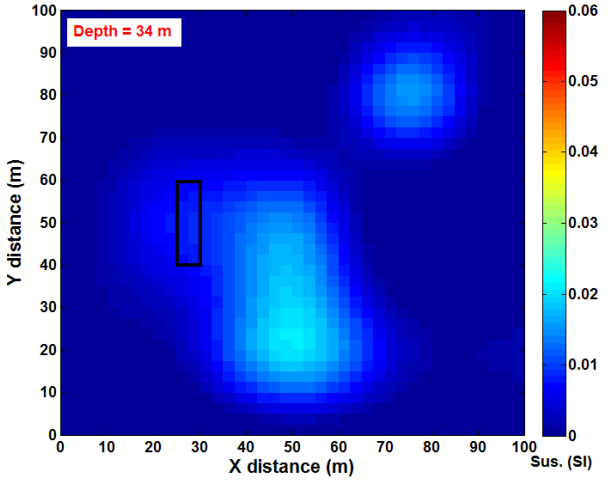

(d)

Figure 5. Horizontal depth slices of the synthetic magnetic susceptibility model shown in Figure 3e for an optimum iteration number of 484. Note that the rectangular borders are the true edges of the synthetic sources

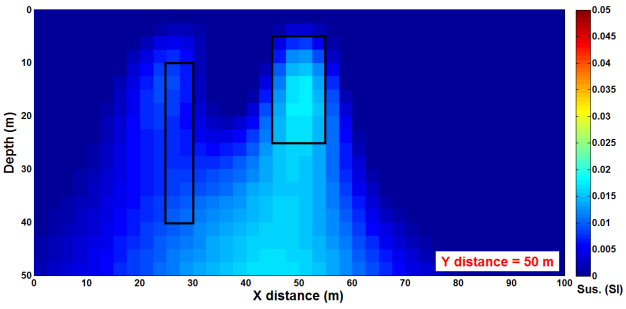

Figure 6. A vertical slice of the magnetic susceptibility model shown in Figure 3e for an optimum iteration number of 484 at Y=50 m. Note that the rectangular borders are the true edges of the synthetic sources

 DOI: https://doi.org/10.30564/jgr.v1i3.1316

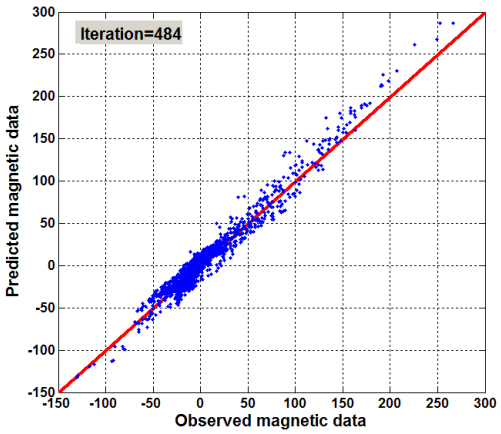

Figure 7. Scatter plot of the predicted data versus the synthetic observations at an optimum iteration number of 484

4. Geological Setting of the Studied Area

The Kalat-e-Reshm district locates in the Semnan province at the north of the center domain of Iran, where it has high potential for occurrences of the porphyry-type sulfide mineralization like Cu. Evidences of the Cu-bearing mineralization are getting stronger since two porphyry Cu deposits exist at the west and the northeast of the studied area, where an airborne geophysical survey has been conducted (Figure 8). The Precambrian metamorphic units in the eastern portions have outcrops. As the oldest rocks in the region, these units have ingredients of mica-schist, amphibolite and gneiss. Note that the surface geological studies have reported the occurrence of the volcanic rocks that are basalt, andesite, rhyolite and dacite units, embedded by a thick sequence of siltstone, sandstone, and conglomerate [5,7].

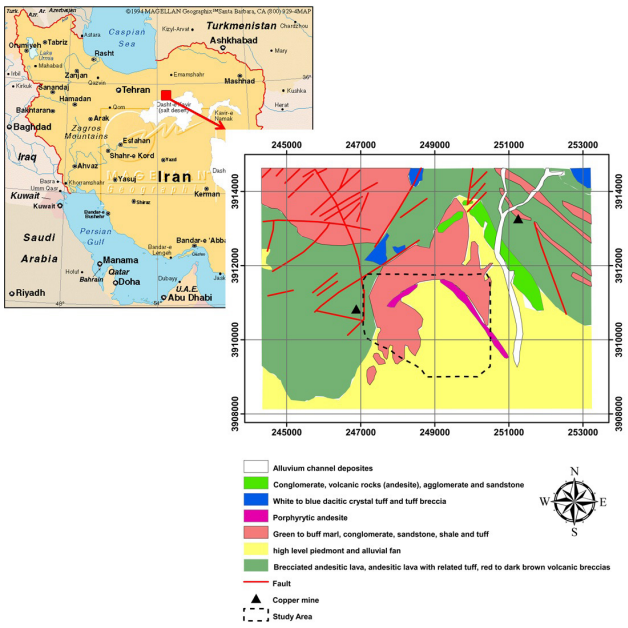

Figure 8. The detailed geology map of the Kalat-e-Reshm area

An arc-shaped porphyritic andesite unit has partially outcropped at the N and NE portions of the area. Erosion phenomenon has removed some parts of this unit at the N regions, whereas the rest part has been covered by unconsolidated soil and alluvium sediment (Figure 8). A distinct sedimentary unit at the north is evident with ingredients of conglomerate, green to buff marl, sandstone, shale and tuff. Both of aforementioned structures are belonged to the Tertiary era. An alluvium channel originates from at the NE and then crosses the meta volcanic structures of the Paleozoic. It contains a mixture of sandstone, conglomerate, tuff, schist, mica-schist, andesitic-basaltic lava, and ultrabasic rocks, accumulated in the shape of high level piedmont and alluvial fans. It covers the arc and continues to the south. The majority of regions have been covered by a composition of sandstone, conglomerate, tuff, shale, marl, and andesitic and volcanic rocks. The region of interest for this study has been outlined by a trapezoid border on the geological map shown in Figure 8. An airborne magnetometry and electromagnetic survey was run by the Geological Survey of Iran in 2003 (GSI) to investigate its mining potential [41,42].

5. Real Case Study for Examining the AIR-RLS Algorithm

The line spacing of the airborne geophysical survey was about 200 m apart, and at an altitude between 30 m and 60 m with respect to the topography. Data were collected at a 4-m spacing along the flight lines to measure the total field magnetic intensity by a cesium magnetometer equipment. After detrending the regional magnetic field, a residual magnetic map is plotted in Figure 9 for 1720 observations. The trace of the sought target, an arc-shaped porphyry andesite unit, is conspicuous. The earth's magnetic field had declination and inclination angles of 3.6° and 53.5°, respectively.

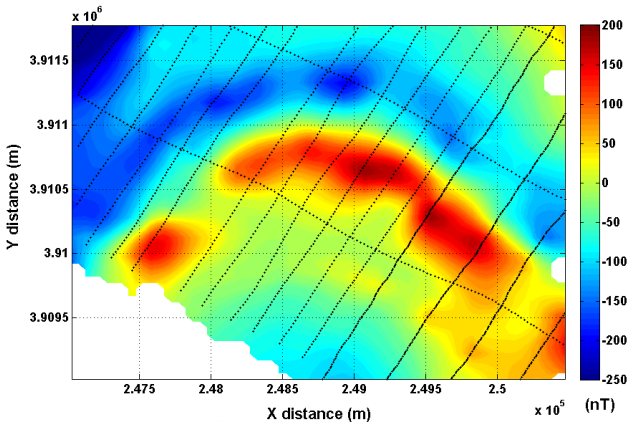

Figure 9. The residual magnetic data over the Kalat-e-Reshm area, where the trace of an arc-shaped porphyry andesite unit is evident

DOI: https://doi.org/10.30564/jgr.v1i3.1316

To run the AIRRLS algorithm, all assumptions for the synthetic magnetic data modeling were considered here again. To perform a 3D magnetic inversion, the model domain was discretized into 34,400 cells (43×40×20) with a uniform dimension of 80×70×20m in the x, y and z directions, respectively. Assuming 500 iterations for running the algorithm, the optimal model was retrieved at iteration 43. The running time of each iteration for 20 PCG iterations was approximately 4.5 s to generate a magnetic susceptibility model. Figure 10 indicates the misfit curve versus the iteration numbers for the real case study. The scatter plot of the predicted data against the magnetic observations has been plotted in Figure 11 with low misfit error..

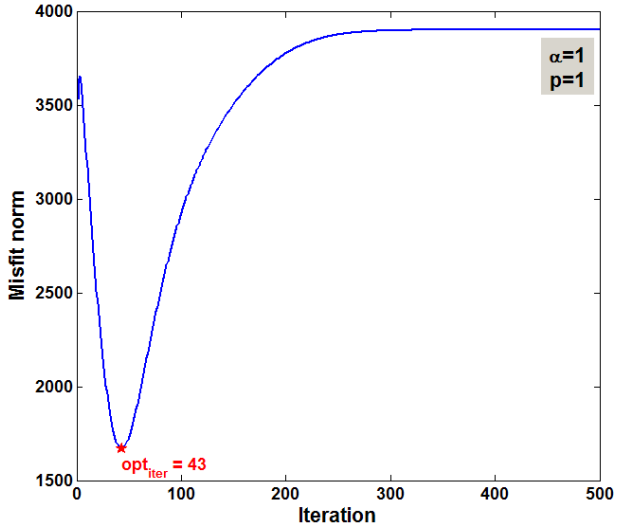

Figure 10. The data misfit versus the iteration numbers for the real magnetic data in the Kalat-e-Reshm area, while an optimum solution was generated at iteration 43

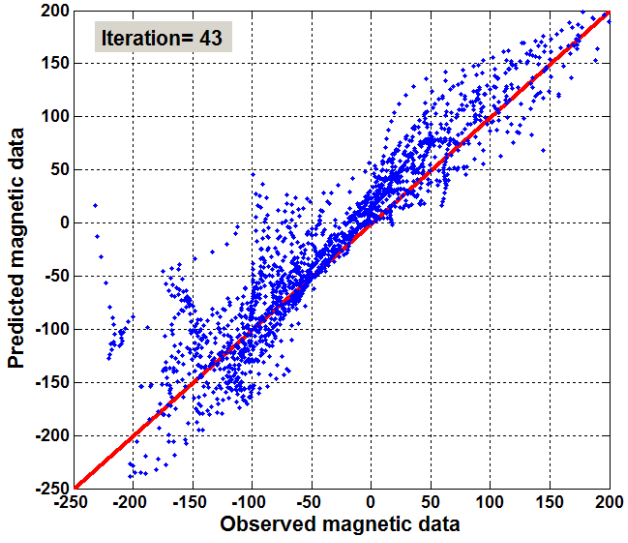

Figure 11. Scatter plot of the predicted data versus the observed airborne magnetic data at an optimum iteration number 43

A 3D rendering of the physical property model at the optimum iteration number has been presented in Figure 12 along eight parallel vertical cross sections that go through the desired sought target. Note that the trace of the arc-shaped unit is conspicuous by its extension at depth. Taking the geological evidences into account accompany with the two porphyry Cu-bearing deposits in the adjacency to this andesite unit, exploratory drilling in this target is highly recommended to investigate its mining potential for Cu occurrences.

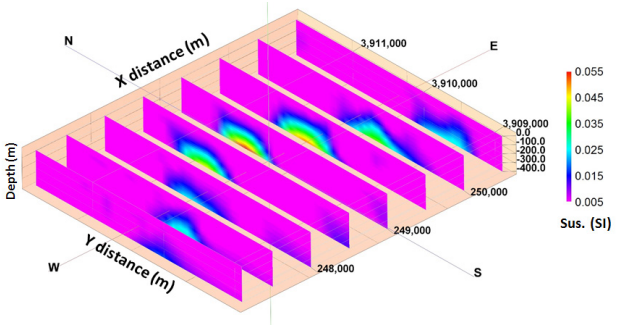

Figure 12. 3D visualization of the magnetic susceptibility model at the Kalat-e-Reshm area through running the AIRRLS algorithm

6. Conclusion

This study has investigated the performance of a fast and automatic algorithm for inversion of magnetometry data. An Augmented Iteratively Re-weighted and Refined Least Squares algorithm (AIRRLS) was run to solve an l_p norm regularization problem in inverse modeling of a magnetic susceptibility property. The algorithm could appropriately recover the magnetic susceptibility model by successively converging to an optimum solution. The significance of this study lies in improvement of the performance of the regularization parameter as a stopping criterion. The applicability of the proposed algorithm was examined for a simulated multi-source magnetic anomaly, and a real case study pertaining to a plausible porphyry copper unit in the Semnan province of Iran. Imaging of an arc-shaped porphyry andesite unit through an airborne survey was the main aim of the prospect to seek its potential for the porphyry Cu-bearing mineralization.

Acknowledgement

The author would like to appreciate the support provided by the School of Mining Engineering, University of Tehran, Iran, and the Geological Survey of Iran (GSI) for providing the processed airborne geophysical data.

 DOI: https://doi.org/10.30564/jgr.v1i3.1316

References

[1] Abdelrahman EM, Essa KS. Magnetic interpretation using a least-squares, depth shape curves method. Geophysics, 2005, 70: L23-L30.

[2] Abdelrahman EM, Essa KS. A new method for depth and shape determinations from magnetic data. Pure Appl. Geophys, 2015, 172: 439-460.

[3] Abedi M, Afshar A, Ardestani VE, Norouzi GH, Lucas C. Application of Various Methods for 2D Inverse Modeling of Residual Gravity Anomalies. Acta Geophys, 2010, 58: 317-336.

[4] Abedi M, Gholami A, Norouzi GH, Fathianpour N. Fast inversion of magnetic data using Lanczos bidiagonalization method. J Appl Geophys, 2013a, 90: 126-137.

[5] Abedi M, Norouzi GH, Fathianpour N, Gholami A. Approximate resistivity and susceptibility mapping from airborne electromagnetic and magnetic data, a case study for a geologically plausible porphyry copper unit in Iran. Journal of Mining & Environment, 2013b, 4: 133-146.

[6] Abedi M, Gholami A, Norouzi GH. 3D inversion of magnetic data seeking sharp boundaries: a case study for a porphyry copper deposit from Now Chun in central Iran. Near Surface Geophysics, 2014, 12: 657-666.

[7] Abedi M, Norouzi GH, Fathianpour N, Gholami A. Geological structure imaging from airborne electromagnetic and magnetic data, a case study in Kalat-e-Reshm area, Iran. Arab J Geosci, 2015, 8: 425-435.

[8] Abedi M, Bahroudi A. A geophysical potential field study to image the Makran subduction zone in SE of Iran. Tectonophysics, 2016, 688: 119-134.

[9] Bhattacharyya BK. Magnetic anomalies due to prism-shaped bodies with arbitrary polarization. Geophysics, 1964, 29: 517-531.

[10] Bhattacharyya BK. A generalized multibody model for inversion of magnetic anomalies. Geophysics, 1980, 29: 517-531.

[11] Boulanger O, Chouteau M. Constraints in 3D gravity inversion. Geophysical Prospecting, 2001, 49: 265-280.

[12] Chasseriau P, Chouteau M. 3D gravity inversion using a model of parameter covariance. J Appl Geophys, 2003, 52: 59-74.

[13] Clark DA. Magnetic petrology of igneous intrusions-Implications for exploration and magnetic interpretation. Exploration Geophysics, 1999, 20: 5-26.

[14] Caratori Tontini F, Cocchi L, Carmisciano C. Depth-to-the-bottom optimization for magnetic data inversion: Magnetic structure of the Latium volcanic region, Italy. Journal of Geophysical Research, 2006, 111: 1-17.

[15] Essa KS. A simple formula for shape and depth determination from residual gravity anomalies. Acta Geophys, 2007a, 55: 182-190.

[16] Essa KS. Gravity data interpretation using the s-curves method. J. Geophys. Eng. 2007b, 4: 204-213.

[17] Essa KS. A new algorithm for gravity or self-potential data interpretation. J. Geophys. Eng. 2011, 8: 434-446.

[18] Gholami A, Mohammadi Gheymasi H. Regularization of geophysical ill-posed problems by iteratively re-weighted and refined least squares. Comput Geosci, 2016.
DOI: 10.1007/s10596-015-9544-1

[19] Gholami A, Siahkoohi HR. Regularization of linear and non-linear geophysical ill-posed problems with joint sparsity constraints. Geophys. J. Int. 2010, 180: 871-882.

[20] Jin SG, van Dam T, Wdowinski S. Observing and understanding the Earth system variations from space geodesy. J. Geodyn. 2013, 72: 1-10.

[21] John DA, Ayuso RA, Barton MD, Blakely RJ, Bodnar RJ, Dilles JH, Gray, Floyd, Graybeal FT, Mars JC, McPhee DK, Seal RR, Taylor RD, Vikre PG. Porphyry copper deposit model, chap. B of Mineral deposit models for resource assessment: U.S., Geological Survey Scientific Investigations Report, 2010, 2010–5070–B: 169 .

[22] Lai M, Wang J. An unconstrained lq minimization with 0<q<1 for sparse solution of under-determined linear systems. SIAM J. Optim. 2011, 21: 82-101.

[23] Last BJ, Kubik K. Compact gravity inversion. Geophysics, 1983, 48: 713-721.

[24] Lelièvre PG, Oldenburg DW. A 3D total magnetization inversion applicable when significant, complicated remanence is present. Geophysics, 2009, 74: L21-L30.

[25] Li Y, Shearer SE, Haney MM, Dannemiller N. Comperhensive approaches to 3D inversion of magnetic data affected by remanent magnetization. Geophysics, 2010, 75: L1-L11.

[26] Li Y, Oldenburg DW. Fast inversion of large-scale magnetic data using wavelet transforms and logarithmic barrier methods. Geophys. J. Int. 2003, 152: 251-265.

[27] Li Y, Oldenburg DW. 3-D inversion of gravity data. Geophysics, 1998, 63: 109-119.

[28] Li Y, Oldenburg DW. 3-D inversion of magnetic data. Geophysics, 1996, 61: 394-408.

[29] Lyu Q, Lin Z, She Y, Zhang C. A comparison of typ-

DOI: https://doi.org/10.30564/jgr.v1i3.1316

ical lp minimization algorithms. Neurocomputing, 2013, 119: 413-424.

[30] Malehmir A, Thunehed H, Tryggvason A. Case History: the Paleoproterozoic Kristineberg mining area, northern Sweden: Results from integrated 3D geophysical and geologic modeling, and implications for targeting ore deposits. Geophysics, 2009, 74: B9-B22.

[31] Namaki L, Gholami A, Hafizi MA. Edge-preserved 2-D inversion of magnetic data: an application to the Makran arc-trench complex. Geophys. J. Int. 2011, 184: 1058-1068.

[32] Oldenburg DW, Li Y, Ellis RG. Inversion of geophysical data over a copper gold porphyry deposit: A case history for Mt. Milligan. Geophysics, 1997, 62: 1419-1431.

[33] Oskooi B, Abedi M. An airborne magnetometry study across Zagros collision zone along Ahvaz–Isfahan route in Iran. Journal of Applied Geophysics, 2015, 123: 112-122.

[34] Pignatelli A, Nicolosi I, Chiappini M. An alternative 3D source inversion method for magnetic anomalies with depth resolution. Ann. Geophys. 2006, 49: 1021-1027.

[35] Pilkington M. 3-D magnetic imaging using conjugate gradients. Geophysics, 1997, 62: 1132-1142.

[36] Portniaguine O, Zhdanov MS. 3-D magnetic inversion with data compression and image focusing. Geophysics, 2002, 67: 1532-1541.

[37] Rao DB, Babu NR. A rapid method for three-dimensional modeling of magnetic anomalies. Geophysics, 1991, 56: 1729-1737.

[38] Shamsipour P, Chouteau M, Marcotte D. 3D stochastic inversion of magnetic data. J Appl Geophys, 2011, 73: 336-347.

[39] Shirzaditabar F, Oskooi B. Recovering 1D conductivity from AEM data using Occam inversion. J Earth Space Phys. 2010, 37: 47–58.

[40] Shirzaditabar F, Oskooi B. Approximate interpretation of airborne electromagnetic data using a half-space model. J Earth Space Phys. 2011, 38: 1-12.

[41] Shirzaditabar F, Bastani M, Oskooi B. Imaging a 3D geological structure from HEM, airborne magnetic and ground ERT data in Kalat-e-Reshm area, Iran. J Appl Geophys, 2011a, 75: 513-522.

[42] Shirzaditabar F, Bastani M, Oskooi B. Study of the effects of the variables changes on the inversion of airborne electromagnetic data in frequency domain. Iranian J Geophys, 2011b, 5: 38-50.

[43] Thoman MW, Zonge KL, Liu D. Geophysical case history of North Silver Bell, Pima County, Arizona-A supergene-enriched porphyry copper deposit, in Ellis, R.B., Irvine, R. & Fritz, F., eds., Northwest Mining Association 1998 Practical Geophysics Short Course Selected Papers on CD-ROM: Spokane. Washington, Northwest Mining Association, 2000, 4: 42 .

[44] Tikhonov AN, Arsenin VY. Solutions of Ill-Posed Problems. Winston, Washington, D. C.

[45] Van Wijk K, Scales JA, Navidi W, Tenorio L (2002) Data and model uncertainty estimation for linear inversion. Geophysics J. Int. 1977, 149: 625-632.

[46] Zhang Y, Yan J, Li F, Chen C, Mei B, Jin S, Dohm JH. A new bound constraints method for 3-D potential field data inversion using Lagrangian multipliers. Geophys. J. Int. 2015, 201: 267-275.

 DOI: https://doi.org/10.30564/jgr.v1i3.1316